MRS Advances © 2018 Materials Research Society
DOI: 10.1557/adv.2018.364

Creating a Novel Graphene Oxide/Iron/Polylactic Acid Composite that Promotes Dental Pulp Stem Cell Proliferation and Mineralization

Rebecca Isseroff[1,2], John Chen[2], Zaiff Khan[2], Anoushka Guha[2], Simon Lin[1], Juyi Li[1], Kuan-che Fang[1], Linxi Zhang[1], Marcia Simon[3], Miriam Rafailovich[1]

[1]*Stony Brook University, Stony Brook, NY 11794, U.S.A.*

[2]*Lawrence High School, Cedarhurst, NY 11516, U.S.A.*

[3]*Stony Brook School of Dental Medicine, Stony Brook, NY 11794, U.S.A.*

ABSTRACT

Dental pulp stem cells (DPSCs) can differentiate into bone cells when provided the correct environment, potentially generating cells to repair non-union fractures. Polylactic Acid (PLA) is a biocompatible polymer for 3-D printing of scaffolds, but DPSCs do not proliferate well on PLA. With the goal of making PLA more conducive for DPSC growth, Graphene Oxide (GO); partially reduced Graphene Oxide (pRGO); GO with iron nanoparticles (FeGO) or Fe-pRGO were incorporated into PLA and spun cast as thin films onto silicon wafers for DPSC plating. DPSCs on Fe-pRGO displayed the fastest doubling time and the highest cell modulus; Fe-pRGO with exterior magnets produced high cell density. SEM demonstrated DPSC mineralization, whereas PLA-only DPSC cultures showed none. Results suggest that PLA/Fe-pRGO and PLA/pRGO enhance DPSC proliferation and possibly differentiation with the potential for use as a 3-D printed scaffold for tissue engineering.

INTRODUCTION

"Nonunion" bone fractures, or breaks that fail to heal, occur in 5-10% of all fracture patients [1]. Bone graft surgery is utilized as an option for repair, but allografts run the risk of rejection and autologous extracted bone grafts take a long time to heal due to multiple surgical sites [2]. Bone loss is also generated by periodontal disease, which causes inflammation leading to bone loss around the tooth or teeth that are surrounded by the infected gum. Jaw bone depletion is a major cause of tooth loss in adults [3]. Teeth replaced by dental implants run the risk of infection, injury or damage to the surrounding teeth, and can also cause nerve damage and/or sinus problems [4].

Dental pulp stem cells (DPSCs) are mesenchymal stem cells which are found in the dental pulp [5]. They are pluripotent and have been shown to differentiate into bone, nerve, and cardiac cells etc., depending on their environment and their substrate. The easy isolation and cryopreservation of DPSCs from extracted third molars or deciduous teeth could provide a source of autologous cells which could regenerate bone in nonunion fractures and/or jaw bone loss [6].

Scaffolds need to be made to cultivate and differentiate DPSCs. Tissue engineers seek to produce surfaces that mimic the extracellular matrix and offer support for the proliferation and differentiation of cells within the scaffold [7]. Polylactic acid (PLA), biodegradable polymer that has received much focus as a synthetic scaffold material for bone fixation devices, can be loaded into a 3D printer to produce biomimetic structures [8]. However, DPSCs plated on PLA do not proliferate well and display a long doubling time. Dexamethasone induces differentiation of DPSCs into osteoblasts as well as other types of cells by expressing the Runt-related transcription factor 2 (Runx2) gene, which controls the time and the amount of DNA produced [9]. However, since this steroid can cause side effects such as increased hair growth, vomiting, depression, and vision problems [10], alternative methods of inducing differentiation are desired.

It has been found that DPSCs deposited on graphene created by chemical vapor deposition have induced osteogenic differentiation [11], and graphene oxide (GO) coated on collagen membranes induced differentiation of mesenchymal stem cells derived from bone marrow into osteoblasts and odontoblasts [12]. In addition, Kotani et al found that a static magnetic field increased differentiation of cells as well as stimulate bone formation in mice [13]; and Green et al found that iron nanoparticles on pRGO were paramagnetic/superparamagnetic, depending on the method of synthesis [14]. Iron and manganese are already being incorporated into 3D printers as biodegradable metal scaffolding to grow bone cells [15].Thus, this project synthesized partially reduced graphene oxide (pRGO) (partial reduction to maintain solubility) and incorporated GO and partially reduced GO into PLA to see if it would stimulate both DPSC growth and mineralization on the composite. Since iron is biodegradable and has magnetic properties that may enhance cell differentiation and proliferation, iron nanoparticles were also incorporated into GO (FeGO) and pRGO (FepRGO) and tested under a static magnetic field by attaching neodymium magnets to the exteriors of some of the iron composite cell cultures. A method was devised to incorporate these graphene oxide derivatives into PLA; GO/PLA, pRGO/PLA, Fe-GO/PLA, and Fe-pRGO/PLA combinations were created and characterized. After spincasting these polymer composites onto silicon wafers, DPSCs were plated on these surfaces and incubated. Cell proliferation and doubling time were measured; cell density and F-Actin amounts were noted; and calcium mineral deposits were identified by scanning electron microscopy and EDS. Thus the goal of this research was to create an enhanced PLA substrate that can be favourable for DPSC growth and mineralization.

EXPERIMENTAL DETAILS

Synthesis: Graphene Oxide (GO), partially Reduced Graphene Oxide (prgo), and Iron-nanoparticles in GO (Fe-GO) and prgo (Fe-prgo)

Graphene oxide was synthesized using a modified Hummer's method [16]. The GO paste was washed repeatedly until the filtrate showed reduced acidity, and then dried in glass vials in a vacuum oven at 45^{o}C. For experiments, solutions of 1 mg/ml GO in distilled water were sonicated for 30 minutes and then centrifuged at 3000 rpm for 25 minutes to separate out remaining graphite and multi-layer sheets. The supernatant was partially reduced with freshly-made sodium borohydride, added to make the final concentration 12 mmolar in $NaBH_4$. Partial reduction removes most but not all GO functional groups [17], leaving the sheets in solution and permitting further functionalization or modification. To make FeGO and Fe-pRGO, 20 drops of iron pentacarbonyl ($Fe(CO)_5$, Sigma-Aldrich, lot #SHBD9102V) from a microsyringe were added to each of two 15 ml GO solutions and allowed to stir overnight. The next day one of the solutions was partially reduced with 12 mM $NaBH_4$ to make Fe-pRGO.

Synthesis and Characterization: Incorporating Graphene Oxide (GO) into Polylactic Acid (PLA)

Of the various common polar organic solvents tested for compatibility between PLA and GO, only ethanol was successful in dissolving both together. However, once this mixture was reduced with $NaBH_4$, pRGO precipitated out. Therefore, 1% by mass dried GO supernatant flakes were added to a chloroform solution containing 3.5mg PLA /mL, sonicated for 45 minutes and then stirred overnight to create uniform suspensions of GO in dissolved PLA. This same technique was done to make PLA mixtures with pRGO; FeGO; and FepRGO. Silicon (Si) wafers were cleaned by rinsing in deionized (DI) water; then boiled for 15 minutes in a 1:1:1 ratio of hydrogen peroxide: sulfuric acid: H_2O and rinsed again in DI water. Films were spuncast at 3000rpm (Headway Research, Model PWM32) and their resulting thicknesses measured in an ellipsometer (Rudolph Research Auto EL) ranged from 50-80nm, the target thickness for plating the DPSCs.

Atomic Force Microscopy (AFM, Brucker DI-3000, SiN3 tip) measured the topography and friction of the films (PLA/GO, and FeGO) before plating and was also used four days after plating to test cell modulus, finding the slope of 9 data points and the average for each group. A silicon wafer with PBS was used as a control. The speed was set at 0.301Hz and the resolution at 512 samples/line. The cantilever (Bruker Model: DNP-10) was coated only on the backside with reflective Au and had a tip of D-fo: 18KHz. Transmission Electron Microscopy [(TEM)JEOL JEM 1400] was used to image Fe nanoparticles on the GO/pRGO carbon sheets. Diameters of 30 Fe nanoparticles were measured using Image J and their values averaged. Scanning Electron Microscopy [(SEM) Leo 1550, Zeiss] was used to investigate for mineralization after 28 days of DPSC growth on each substrate.

Application: Plating Dental Pulp Stem Cells (DPSCs)

Cut Si wafers were cleaned by boiling for 15 minutes in 1:1:1 H_2O_2:H_2SO_4:H_2O, and washed in H_2O. The wafers were spun-cast with composite test solutions to produce films of PLA/GO, PLA/FeGO without a magnetic field, and PLA/FeGO subjected to an exterior magnetic field of neodymium magnets mounted above and below the culture plates. Si wafers were prepared to analyse for doubling time, SEM, confocal microscopy, and cell modulus. The wafers were annealed over the weekend at 40-50 ^{o}C in a vacuum oven to drive off the solvents but to avoid degrading the GO at higher temperatures. This process was repeated to coat Si wafers with PLA (control), PLA/pRGO, PLA/Fe-pRGO, and PLA/Fe-pRGO with magnets. A Rudolph Research Auto EL ellipsometer determined the thickness of the PLA film containing GO particles to be about 70-80 nanometers thick, while the film with only PLA was about 50 nanometers thick.

DPSCs (Strain AV3) were grown in MEM alpha supplemented with 10% fetal bovine serum (FBS, HyClone) and ascorbic acid. At 70-90% confluence, cells were detached from the tissue culture plate with Trypsin/EDTA (Gibco), followed by neutralization of trypsin with medium. Cells were collected by centrifugation at 500 x g and then were plated at 1.5 x 10^4 cells or 3 x 10^4 cells per well using 12-well and 6-well plates, respectively. Cultures were incubated at 37^{o}C, 7% CO_2 in MEM alpha supplemented with 10% FBS, ascorbic acid and beta-glycerol phosphate. Media was changed every 2-3 days. For PLA/Fe-GO and PLA/Fe-pRGO with exterior magnetics, the 6-well plates were incubated between two trays of magnets starting on day 1.

To fix and stain the cells for confocal microscopy, media from the wells was aspirated and the wells were rinsed twice with PBS. Then, 2 ml of 10% formalin were added to each well and kept for 20 minutes; then aspirated and the wells rinsed once with PBS and fresh PBS was added. Then, added in succession to the cells were 4% Triton in PBS incubated for 7.5 minutes to permeabilize the cells; 5 µm Alexa Fluor per 1 mL PBS for 20 minutes to stain for Fiber-actin; and 4',6-diamidino-2-phenylindole (DAPI) for 3 minutes to stain for nuclei; washing twice with PBS between each type of stain.

RESULTS

Atomic Force Microscopy (AFM) for Film Characterization

The spun cast films were first characterized using AFM in both topography and friction modes. The topographical and friction images for the GO and FeGO samples are shown in figure 1. From the figure we can see that the films are relatively flat and have "wet", meaning they have completely coated the Si wafers even after high-temperature annealing. In both cases the friction images reveal the distribution of the GO and the FeGO particles within the films, which are harder than the surrounding polymer matrix and hence have good friction contrast. Furthermore, these scans indicate that the GO and FeGO particles are near the film surface and are therefore able to modify its charge distribution in electrolyte solutions.

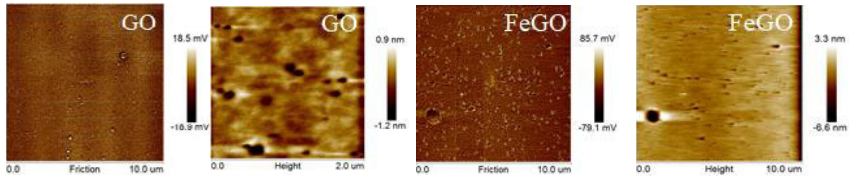

Figure 1. AFM friction and topography images, respectively, of (left) GO in PLA and (right) FeGO in PLA

Transmission electron microscopy (TEM)

As shown in Figure 2, the GO is visible as sheets while the Fe-pRGO has nanoparticles evenly dispersed throughout its structure. The diameters of thirty Fe nanoparticles were measured using the program Image J; average diameter was calculated to be 6.1 nm (s.d 1.90).

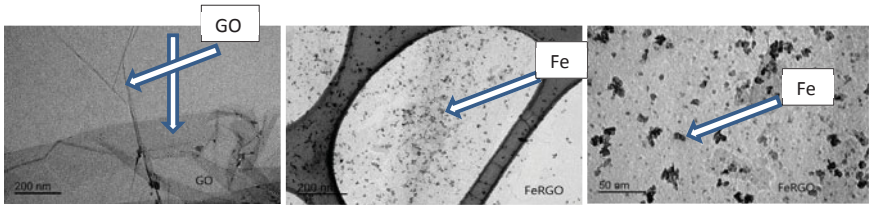

Figure 2. TEM images of (left) GO sheets; (center) Fe-pRGO; and (right) Fe-pRGO under higher magnification, where the Fe particles, having higher electron density, appear dark.

Cell doubling time

DPSCs incubated on Si wafers spuncast with thin films of PLA alone; PLA/GO; PLA/FeGO; PLA/pRGO; and PLA/FepRGO were counted on days 1, 2, and 3, and graphed to compare growth rates (Figure 3). PLA/Fe-pRGO displayed the fastest cell doubling time of any of the samples, although both PLA/GO and PLA/pRGO also exhibited shorter cell doubling times as compared to the PLA.

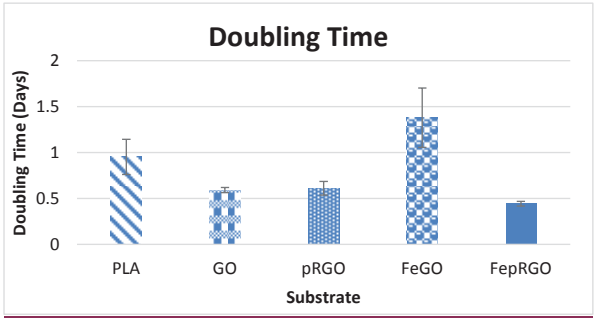

Figure 3. DPSC doubling time as measured from hemocytometer readings after 24, 48, and 72 hours in culture.

Cell Modulus and Relative Modulus

Previous research found that adipose-derived stem cells with higher elastic modulus had greater potential for osteogenesis [18]. As shown in Figure 4, cell moduli after 4 days of growth on the reduced substrates were harder than the cell moduli on plain PLA. PLA/Fe-pRGO without magnets had the most rigid cells, displaying a 71% higher modulus than cells on PLA, and PLA/Fe-pRGO-Mag had the second highest modulus, 37% higher compared to PLA. Unreduced substrates produced cell moduli >100 times softer, indicating that pRGO and GO exert different effects on the cells.

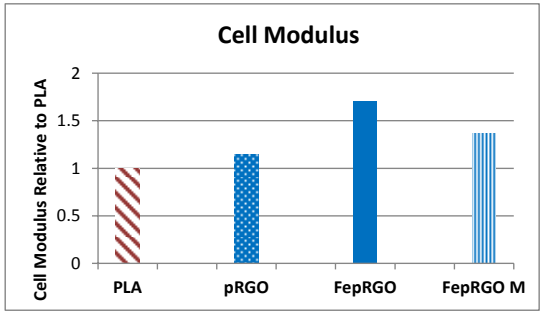

Figure 4. Relative Cell Modulus of DPSCs on reduced substrates; Modulus compared to PLA, set as =1.

Confocal Microscopy after 14 days of Incubation

After 14 days of incubation, few DPSCs were observed on the PLA surfaces. In contrast as we can see in Figure 5, PLA nanocomposites with GO, pRGO, Fe-GO, Fe-GO-Magnets, and Fe-pRGO, substrates displayed high cell density and confluence.

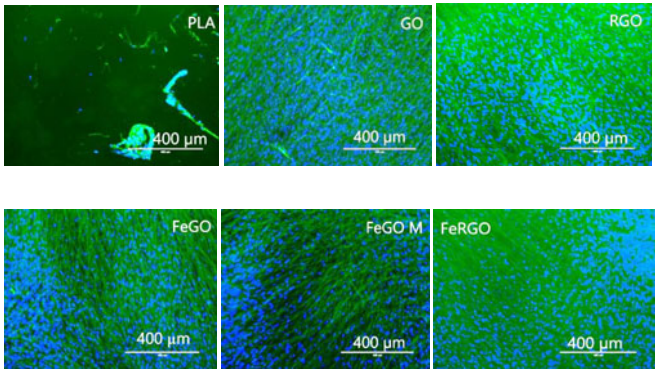

Figure 5. Confocal Microscope images of DPSCs after 14 days of incubation on (top, starting from left) PLA; GO; RGO; (bottom, starting from left) FeGO; FeGO-M; and Fe-pRGO (10K magnification). F-actin is stained green with Alexafluor-Phalloidin-488 and the nuclei are stained blue with DAPI.

Confocal Microscopy after 28 days of Incubation

After incubating the cells on the substrates for 28 days, a modest increase in cell number was observed on the PLA control (Figure 6). However, all test substrates display a high cell density where more f-actin (which promotes processes such as motility, cell division and cell signalling) is observed than for the cells on the PLA control (figure 6). On all the other substrates, except for PLA, the cells are well extended indicating the formation of tissue. In fact, cells seem to have fallen off the pRGO substrate during fixing and staining because so many cells had grown that, the tissue had become sufficiently thick that it had started to detach from the substrate as a single sheet.

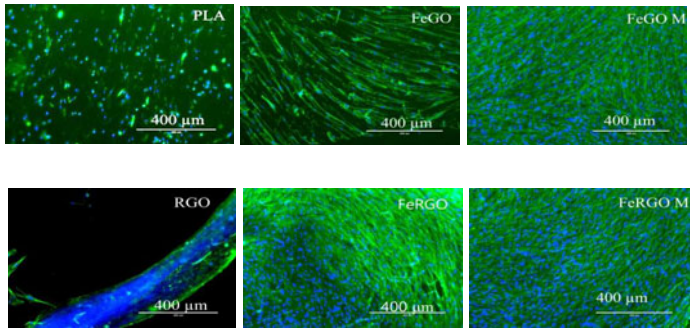

Figure 6. DPSCs after 28 days of incubation on: (top) PLA, FeGO, FeGO-M; (bottom) pRGO, Fe-pRGO, and Fe-pRGO-Magnets (10K magnification) **All test samples show greater cell density and F-Actin than PLA control** (except for RGO which lifted off of the wafer as tissue during washing). F-actin is stained green with Alexafluor-Phalloidin-488 and the nuclei are stained blue with DAPI.

Scanning Electron Microscopy (SEM) and Energy Dispersive X-Ray Spectroscopy (EDS)

After 28 days of cell incubation on the substrates, SEM investigated for cell mineralization and the elemental composition of the minerals was identified by Energy Dispersive X-Ray Spectroscopy (EDS). Initially the PLA wafer was not washed correctly, leaving soluble salts on the silicon (figure 7). However, EDS showed the PLA still had no detectable calcium or phosphorous deposited by DPSCs; only high peaks of sodium and chlorine. However, all PLA/GO/pRGO test substrates show mineralization (figure 8). EDS identifies peaks of calcium and phosphorous in the minerals, suggesting that these deposits are made of calcium phosphate. FepRGO-M showed a significantly lower Ca peak than P, raising questions about the quality of its mineralization as compared to the other test substrates which display high Ca/P peaks.

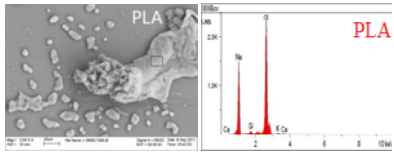

Figure 7. SEM (left) magnified at 3.0 K X of minerals on PLA-only substrate after DPSCs had grown for 28 days. EDS (right) shows PLA had mostly Na and Cl, left from improper rinsing

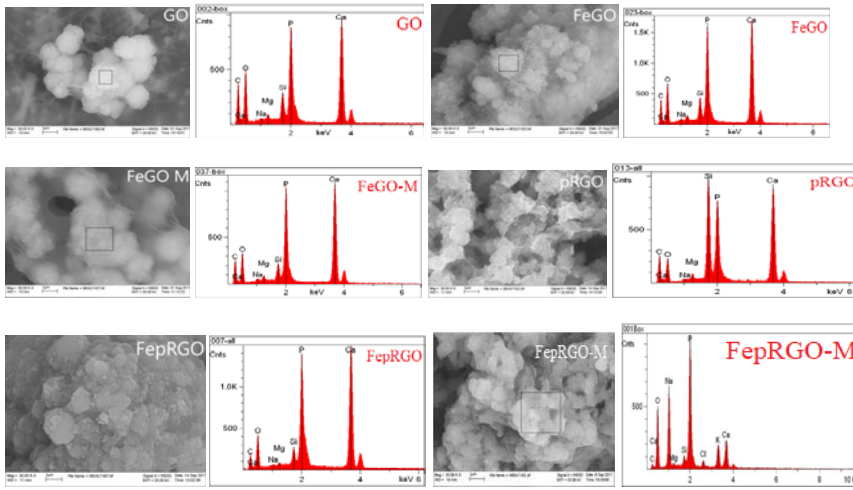

Figure 8. SEM images taken at 30.0 K X of minerals deposited on the test substrates after DPSCs had grown for 28 days. EDS obtained from the areas in the square region shown in the figures, display high peaks of Ca and P on every test substrate.

DISCUSSION

Cells that make up tissues attach to the extracellular matrix and to neighbouring cells, with the matrix mechanics affecting the ability of the cell to attach and proliferate. Generally speaking, cells prefer a stiffer matrix on which they produce more organized cytoskeletons and more stable focal adhesions [20]. This research has shown that polylactic acid (PLA) cannot alone act as an efficient substrate that will grow DPSCs or cause them to differentiate, although it is not known whether this is because PLA does not provide the required modulus or because, as a mostly hydrophilic polymer, it does not offer sufficient charge for DPSC adhesion and growth. PLA was mixed with 1% by mass GO (relative to PLA), GO+Fe nanoparticles, and their partially reduced counterparts to produce composites of PLA that were tested as substrates for DPSC growth and mineralization. TEM confirmed that the Fe samples had dispersed iron nanoparticles averaging 6 nanometers in diameter. DPSCs were plated onto the different composite PLA substrates and incubated without the use of dexamethasone, a steroid normally used to induce differentiation. DPSCs plated on PLA/pRGO, PLA/Fe-pRGO, and PLA/Fe-pRGO with an exterior magnetic field caused the DPSC modulus to increase relative to PLA. This is significant since it has been shown that mechanical stiffness is an indicator of early stem cell differentiation [19]. Cell doubling time was faster on almost all test substrates relative to PLA. Cells plated on Fe-pRGO doubled twice as fast as cells plated on PLA. Both Fe-GO-magnets and Fe-pRGO-magnets showed high cell density in confocal microscope images, signifying a magnetic field coupled with paramagnetic iron particles could generate favorable conditions for cell growth. These results suggest that not only are iron nanoparticles nontoxic to DPSCs when added to GO/pRGO, but they *enhance* DPSC growth.

After 28 days of DPSC incubation, SEM visualized cell mineralization on the washed substrates and confirmed with EDS the presence of calcium and phosphorous, two elements found in hydroxyapatite which makes up bone structure and gives it rigidity. However, to signify hydroxyapatite, the calcium peak should be higher than the phosphorous peak, but the FepRGO-M has a much shorter Ca peak, hinting that this may not be hydroxyapatite. It is interesting to note that all the other test substrates, including FeGO-M, have a high Ca peak along with the P peak. This finding suggests that the application of an exterior magnetic field to the combination of PLA/FepRGO has a negative effect on the mineralization of the DPSCs, while the application of an exterior magnetic field does not impede the mineralization on PLA/FeGO. Again,

it is unclear whether the test substrates enhance DPSC growth and proliferation due to increasing the charges in the PLA, or because adding these particles to PLA increases its modulus, making it more hospitable for cell adhesion and growth. In the future, RT-PCR will be conducted to look for Osteocalcin, DSPP, and Alkaline Phosphatase, three proteins that signify that the DPSCs are differentiating and that the calcium phosphate deposits seen on SEM are due to differentiation and biomineralization without the use of dexamethasone.

From the atomic force microscopy images we observed that the graphene oxide and reduced graphene oxide particles were near the film surface. Cells do not have receptors for polymeric materials, but can recognize functional domains exposed on extracellular matrix proteins. Therefore, in order for cell adhesion to occur it must be preceded by protein adsorption and the plating efficiency will be very sensitive to the conformation of the adsorbed proteins. In this case, we found that PLA did not support cell adhesion and hence the plating efficiency was poor. Cell proliferation was poor even after 14 days in culture, and a limited amount of cells were observed only after 28 days. However, simply with the addition of the various graphene oxide nanoparticles, a striking and immediate change was observed within the first 24 hours. The plating efficiency increased drastically, and good tissue formation was seen at 14 days in culture. These results occurred within the first few hours after plating, indicating that they were not initiated by upregulation of any specific mechanism in the cell. Rather, the presence of the particles at the film surface modified the initial adsorption of serum proteins onto the PLA surface which enabled cell adhesion, increased plating efficiency and encouraged subsequent ECM protein deposition. Furthermore, since serum proteins are diamagnetic, Ba et al [21] showed that their adsorption is also influenced by moderate magnetic fields, such as those used in this study. Even though we were unable to directly observe their morphology, as reported in ref. 21, we were able to detect differences in the nature of the mineral deposition in the presence of an external magnetic field. Ba et al showed that mineral deposition was templated onto the surface-adsorbed proteins in vitro, and hence any change in the protein conformation affected the nature of the deposits. In that study, the external field increased the degree of crystallinity of the minerals produced by mouse 3T3 cells, while in our case it appears that the magnetic field decreases the calcium content of the deposits produced by human DPSCs. Therefore, in the case of human DPSCs it seems that the increased charge content enhances DPSC proliferation and hydroxyl apatite mineral deposition, but the additional presence of an external magnetic field may reverse the beneficial aspect of the surface charge.

With more development and testing, an application of this work could be that DPSCs can be taken from deciduous teeth or extracted wisdom teeth and frozen for future autologous stem cell transplants. A PLA/Fe-pRGO composite can be loaded into a 3D printer, producing a scaffold for the cells that can produce tissue which can then be implanted back into the patient's body to alleviate bone loss or repair non-union fractures.

ACKNOWLEDGMENTS

The authors would like to thank the National Science Foundation Project Inspire and the Morin Foundation for their support of this research.

At the date this manuscript was written, URLs or links referenced herein were deemed to be useful supplementary material to this manuscript. Neither the authors nor the Materials Research Society warrants or assumes liability for the content or availability of URLs referenced in this manuscript.

REFERENCES

1. R. Zura, Z. Xiong, T. Einhorn, J.T. Watson, R.F. Ostrum, M.J. Prayson, G.J. Della Rocca, S. Mehta, T. McKinley, Z. Wang, and R.G. Steen: *Epidemiology of Fracture Nonunion in 18 Human Bones*. JAMA Surgery, **Vol. 105**, pp.e162775, doi:10.1001/jamasurg.2016.2775, (2016).

2. *Nonunions* (2014). Available at: orthoinfo.aaos.org/topic.cfm?topic=A00374 (accessed 1 September 2017)

3. D.L Cochran: *Inflammation and Bone Loss in Periodontal Disease*. Journal of Periodontology, **Vol 79**, pp. 1569-1576, doi:10.1902/jop.2008.080233, (2008).

4. *Dental Implant Surgery* (2016). Available at: www.mayoclinic.org/tests-procedures/dental-implant-surgery/details/risks/cmc-20245747. (accessed 3 September 2017)

5. R. Nasser: *Stem Cells from Dental Pulp Used to Make Corneal Cells* (2015). Available at: http://palmbeachdentistfl.com/ (accessed 4 September 2017)

6. M. Tatullo, M. Marrelli, K.M. Shakesheff, and L.J. White: D*ental Pulp Stem Cells: Function, Isolation and Applications in Regenerative Medicine*. Journal of Tissue Engineering and Regenerative Medicine, **Vol. 9**, pp.1205-1216, doi: 10.1002/term.1899, (2014).

7. A.V. Do, B. Khorsand, S.M. Geary, and A.K. Salem: *3D Printing of Scaffolds for Tissue Regeneration Applications*. Advanced Healthcare Materials, U.S. National Library of Medicine, **Vol. 4**, pp. 1742-1762, doi: 10.1002/adhm.201500168, (2015).

8. M. Savioli Lopes, A.L. Jardini, and R. Maciel Filho: *Poly (Lactic Acid) Production for Tissue Engineering Applications*. *Procedia Engineering*, **Vol. 42,** pp. 1402-1413, doi:10.1016/j.proeng.2012.07.534, (2012).

9. F. Langenbach, and J. Handschel: Effects of Dexamethasone, Ascorbic Acid and β-Glycerophosphate on the Osteogenic Differentiation of Stem Cells in Vitro." Stem Cell Research and Therapy, **Vol. 4**, pp. 117, doi: 10.1186/scrt328, (2013).

10. "Dexamethasone Oral (2017)." Available at: medlineplus.gov/druginfo/meds/a682792.html. (accessed 11 September 2017)

11. H. Xie, M. Chua, I. Islam, R. Bentini, J.C. Viana-Gomes, A.H. Castro Neto, and V Rosa: *CVD-Grown Monolayer Graphene Induces Osteogenic but Not Odontoblastic Differentiation of Dental Pulp Stem Cells*. Dental Materials, **Vol. 33**, pp. E13-e21, doi:10.1016/j.dental.2016.09.030, (2017).

12. M. Radunovic, M. De Colli, P. De Marco, C.Di Nisio, A. Fontana, A. Piattelli, A. Cataldi, and S. Zara: Graphene Oxide Enrichment of Collagen Membranes Improves DPSCs Differentiation and Controls Inflammation Occurrence. Shibboleth Authentication Request, J Biomed Mater Res A., **Vol. 105**, pp. 2312-2320, doi: 10.1002/jbm.a.36085, (2017).

13. H. Kotani, H. Kawaguchi, T. Shimoaka, M. Iwasaka, S. Ueno, H. Ozawa, K. Nakamura, and K. Hoshi: *Strong Static Magnetic Field Stimulates Bone Formation to a Definite Orientation In Vitro and In Vivo*. Journal of Bone and Mineral Research, **Vol. 17**, pp. 1814-1821, doi:10.1359/jbmr.2002.17.10.1814, (2002).

14. A. Green, R. Isseroff, S. Lin, L. Wang, and M. Rafailovich: (2017). Synthesis and characterization of iron nanoparticles on partially reduced graphene oxide as a cost-effective catalyst for polymer electrolyte membrane fuel cells. MRS Communications, **Vol. 7**, Issue 2, pp. 166-172, doi:10.1557/mrc.2017.14, (2017).

15. H. Milkert: *3D Printed Biodegradable Metal Bone Scaffolding Created* (2014): 3DPrint.Com | The Voice of 3D Printing / Additive Manufacturing, 3DR Holdings, Available at: 3dprint.com/1604/3d-printed-biodegradable-metal-bone-scaffolding-created/.

16. W.S. Hummers, and R.E. Offeman: *Preparation of Graphitic Oxide*. Journal of the American Chemical Society, **vol. 80**, pp. 1339, doi:10.1021/ja01539a017, (1958).

17. R. Isseroff, B. Akhavan, C. Pan., H. He., J. Sokolov, and M. Rafailovich: *Enhancing the Efficiency of a PEM Hydrogen Fuel Cell with Synthesized Metal-Nanoparticle/Graphene Composites Synergy*. MRS Proceedings,**Vol. 1658,** rr.15-rr26, doi:10.1557/opl.2014.415, (2014).

18. R.D. González-Cruz, V. C. Fonseca, and E. M. Darling: *Cellular Mechanical Properties Reflect the Differentiation Potential of Adipose-Derived Mesenchymal Stem Cells*. Proceedings of the National Academy of Sciences, vol. 109, pp.E1523-E1529, doi:10.1073/pnas.1120349109, (2012).

19. T. Bongiorno, J. Kazlow, R. Mezencev, S. Griffiths, R. Olivares-Navarrete, J. F. McDonald, Z. Schwartz, B. D. Boyan, T. C. McDevitt, and T. Sulchek: *Mechanical Stiffness as an Improved Single-Cell Indicator of Osteoblastic Human Mesenchymal Stem Cell Differentiation*. Journal of Biomechanics, **vol. 47,** pp. 2197-2204, doi:10.1016/j.jbiomech.2013.11.017, (2015).

20. D.E. Discher, P. Janmey, Y.L. Wang. *Tissue cells feel and respond to the stiffness of their substrate*. Science **310**, 1139 doi: 10.1126/science.1116995 (2005).

21. X. Ba, M. Hadjiargyrou, E. Dimasi, Y. Meng, M. Simon, Z. Tan, and M.H. Rafailovich, *The role of moderate static magnetic fields on biomineralization of osteoblasts on sulfonated polystyrene films.* Biomaterials. 2011 Nov;32**(31)**:7831-8. doi: 10.1016/j.biomaterials.2011.06.053. Epub 2011 Aug 4.